EXPERIMENTAL AND THEORETICAL STUDY OF TWO-PHASE HEAT PIPE

Asst.Prof. Dr.Karima Esmail Amori **Muhanad Latif Abdullah**
Mechanical Engineering Department
University of Baghdad
drkarimaa@yahoo.com kamer_2002@yahoo.com

ABSTRACT

In this study, thermal characteristics of a two-phase closed heat pipe were investigated experimentally and theoretically. A two-phase closed heat pipe (copper container, Fluorocarbon FC-72 (C_6F_{14}) working fluid) was fabricated to examine its performance under the effect of input heat flux range of 250–1253 W/m^2, 70% fill charge ratio and various tilt angles. The temperature distribution along the heat pipe, input heat to evaporator section, and output heat from condenser were monitored. A comprehensive mathematical model was developed to investigate the steady-state heat transfer performance of a two-phase closed heat pipe. A steady state analytical model, is presented to determine important parameters on the design of two-phase closed heat pipe, including temperature levels and heat transfer coefficients for condenser and evaporator. The experimental and simulation results of this work are found in good agreement. The experimental boiling heat transfer coefficients were compared with existing previously reported correlations.

KEYWORDS: heat pipe; solar; thermosyphon; experimental test.

دراسة عملية ونظرية لأنبوب حراري ثنائي الطور

أ.م.د. كريمة اسماعيل عموري
قسم الهندسة الميكانيكية
قسم الهندسة الميكانيكية

مهند لطيف عبدالله
قسم الهندسة الميكانيكية
جامعة بغداد/طالب دكتوراه

الخلاصة:

تم في هذه الدراسة التحقيق عمليا ونظريا في المواصفات الحرارية لأنبوب حراري ثنائي الطور. تم تصنيع انبوب حراري مغلق (حاوية من النحاس ومائع تشغيلي فلوروكاربون) لفحص أداءه بتأثير مدى فيض حراري مسلط عليه يتراوح بين (250 الى 1253 واط/م^2) ، 70% نسبة شحن وعند زوايا ميل مختلفة. تم تحديد توزيع درجات الحرارة على جدار الأنبوب الحراري ، كمية الحرارة الداخلة الى المبخر وكمية الحرارة الخارجة من المكثف.

وضع نموذج رياضي شامل لدراسة أداء النقل الحراري المستقر على انبوب حراري مغلق وثنائي الطور. تم عرض نموذج تحليلي لدراسة تأثير عوامل مهمة على تصميم الأنبوب الحراري، وتضم مستوى درجات الحرارة ومعامل انتقال الحرارة للمكثف والمبخر. وجد توافق جيد بين النتائج التجريبية والنظرية. كما قورنت النتائج التجريبية لمعامل انتقال الحرار للغليان مع علاقات متوفرة في الأدبيات السابقة.

الكلمات الرئيسية: انبوب حراري، شمسي،ثرموسيفون، فحص مختبري.

INTRODUCTION

Due to high fuel prices, it has become necessary to investigate new methods for saving and more efficient use of energy. For this reason, in the last five decades there has been an important technological development in heat transfer equipment, to promote changes in configuration and applying heat transfer systems with high effectiveness. One example is the use of two-phase thermosyphons **(Reay (1981); Azada et. al.(1985);Peterson (1994); Faghri(1995); Gershuni et. al.(2004); Noie(2005))**.

Thermosyphon is a device with high thermal conductivity that can transfer high quantities of heat. In its most simple form, a thermosyphon is a hollow evacuated metal pipe, charged by a pre-determined amount of an appropriate working fluid. It can be divided into three main sections: evaporator, where the heat is delivered to the device, an adiabatic section (which may or may not exist) and a condenser, where the heat is released. The working fluid located in the evaporator, evaporates and go toward the condenser region, where it condenses, returning to the evaporator by means of gravity.

(Streltsov(1975)) developed a correlation of filling ratio as a function of geometry, thermophysical properties of working fluid and heat flux, based on Nusselt theory on condensation in a vertical plate. However, this model assumed that the liquid film thickness was zero at the bottom of evaporator with no consideration to the liquid pool in the evaporator and the interfacial shear stress between liquid film and vapor flow, which makes the calculation much smaller than the real situation. **(Shiraishi et. al. (1981))** developed a simple model when the liquid film and liquid pool are continuous, based on the empirical heat transfer correlations from his experimental results. It can only determine the temperature distribution at the inside wall of thermosyphon, and cannot confirm the location of liquid film and liquid pool inside the thermosyphon. **(Basran et. al.(1985))**solved two-dimensional numerical models in the vertical heated and cooled sections of a thermosyphon loop using uniform wall temperature boundary condition. Results for laminar flow case were obtained by solving the momentum and the energy equations through the SIMPLEX Algorithm. **(El-Genk et. al.(1999), Jialun et. al.(1992))**determined the height of liquid pool by their empirical correlations, some of authors consider one or two forms in their models, and another neglect the height of liquid pool. **(Park et. al.(2002))** studied the heat transfer characteristics in thermosyphon depending on the amount of working fluid and when the operation limits occur. The two-phase element was made of copper and as working fluid FC-72 (C_6 F_{14}) was used. The thermosyphon was subjected to a heat supply in the range of 50-600 W and with FR 10-70%. For the heat transfer coefficients in the condenser and in the evaporator, the authors used the theory of Nusselt and Roshenow respectively. They found that the operation limits manifest in different forms depending on the filling ratios of the fluid. For small filling ratio (FR = 10%) the drying limit occurs in the evaporator, while for high filling ratio (FR = 50%) the flooding limit appears. In the first case, evaporator temperature increases from the evaporator bottom; in the second case the evaporator temperature increases at the top of the evaporator. These conclusions were made by observing the temperature distribution along the thermosyphon. **(Zuo et. al.(2002))** conducted an analytical and experimental research on the thermodynamic behavior of the working fluid in a thermosyphon and a heat pipe, using a temperature-entropy diagram. The authors divide the thermodynamic processes into two categories: 1) heat transfer by conduction through the tube wall and 2) heat and mass transfer, by convection inside the two-phase thermosyphon. **(Noie, (2005))** presented in his work an experimental study of a thermosyphon of (980 mm length and 25 mm internal diameter) made of smooth copper tube, with distilled water as a working fluid. The goal of the study was to

obtain the thermal characteristics of the thermosyphon (temperature distribution in the outer wall along the tube, boiling heat transfer coefficient and the maximum heat transfer rate), at: heat supply ($100 < Q < 900$ W), filling ratios ($30\% \leq FR \leq 90\%$) and length of the evaporator (varying the length of electrical resistance).

The heat transfer performance of a thermosyphon is significantly affected by geometry, inclination angle, vapor temperature and pressure, filling ratio and thermophysical properties of working fluid. For different heat transfer rates and filling ratios, there are three types of flow pattern and two types of transition according to the distribution of liquid film and liquid pool in the thermosyphon. The flow patterns are: (1) liquid film in evaporator dries out; (2) liquid film and liquid pool are continuous (3) liquid pool exceeds the evaporator, while two transitions are: (1) the liquid film thickness in evaporator reaches the minimum value, below which liquid film could dry out, and (2) liquid pool fills the entire evaporator **(Jiao et. al. (2008))**.

Nkwetta et al. (2012) compared experimentally the performance of concentrated and unconcentrated heat pipe solar collector for medium temperature applications. The concentrated type showed an improvement of 25.42% in total daily energy collection. **Fu et al. (2012)** presented a hybrid system of heat pump with heat pipe photovoltaic/thermal collector. They conducted a series of experiments in Hong Kong to study the performance of this system. **Nemec et al. (2013)** proposed and verified a mathematical model for calculating heat transport limitations of heat pipe with various working fluids operating at temperatures from -30^{o}C to 140^{o}C.

The main objective of the present study is to build a theoretical model to predict the steady state thermal behavior of a heat pipe. Moreover, it includes an experimental study to investigate the effect of subjected heat flux, and tilt angle on the heat pipe performance; these objectives can be a comprised by the following:

1. Study the effect of actual evaporator length on the thermal behavior of a heat pipe.
2. Study the effect of using FluoroCarbon FC-72 as a working fluid on the thermal performance of heat pipe.

THEORY

Thermosyphon is divided into three regions: evaporator, condenser and adiabatic section. The condenser and adiabatic section are subdivided into two parts: the region of liquid film and the vapor nucleus. The region of evaporator contains these two volumes plus a liquid pool. Steady state and uniform temperature distributions within the wall (radial direction) of the evaporator and condenser are considered.

CONDENSER

It is assumed that the working fluid (FC-72) is a saturated vapor (single phase) when it reaches the condenser. The condensate which flows back down along the pipe is assumed to be laminar flow with respect to the radius of the thermosyphon. Using Nusselt's film condensation theory for a flat plate **(Incropera et.al. 1990)**, the condensation heat transfer coefficient (h_c) is given by

$$h_c \frac{\left(\frac{\nu^2}{g}\right)^3}{k_l} = \left(\frac{4}{3}\right)^{\frac{1}{3}} (Re_c)^{\frac{-1}{3}} \quad (1)$$

$$Re_c = \frac{4 q_c L_c}{h_{fg} \mu} \quad (2)$$

where

h_c condenser heat transfer coefficient ($W/m^2.K$).
Re_c film Reynolds number (Kg/N).
q_c heat flux at the condenser (W/m^2).
L_c condenser length (m).
h_{fg} latent heat of vaporization (J/kg).
ν kinematic viscosity $=\mu/\rho$ (m^2/s).
μ dynamic viscosity ($N.s/m^2$).

k_l liquid thermal conductivity (W/m.K).
g gravitational acceleration (m/s²).

Adiabatic Section

In the adiabatic section, the equations derived from the Nusselt analysis cannot be applied, because there is no radial heat transfer and the axial heat conduction is relatively small. The thickness of the liquid film is considered constant in this region.

Evaporator

The mean heat transfer coefficient of nucleate boiling in the liquid pool in the evaporator is reported by **(Shiraishi et. al. (1981))** as:

$$h_p = 0.32 \frac{\rho_l^{0.65} k_l^{0.3} C_p^{0.7} g^{0.2}}{\rho_v^{0.25} h_{fg}^{0.4} \mu^{0.1}} \left(\frac{p_{sat}}{p_a}\right)^{0.23} q_e^{0.4} \quad (3)$$

while the correlation of mean heat transfer coefficient given by **(Rohsenow apude Noie (2003))**, is:

$$h_p = \frac{q_e^{2/3}}{\frac{C_{sf} h_{fg}}{C_p}\left\{\frac{1}{h_{fg}\mu_l}\left(\frac{\sigma}{g[\rho_l - \rho_v]}\right)^{0.5}\right\}^{0.33} p_r^{1.7}} \quad (4)$$

where
h_p evaporator pool heat transfer coefficient ($W/m^2.K$).
q_e input heat flux in evaporator (W/m^2).
C_{sf} constant that depended upon the nature of the surface–fluid combination.
C_p specific heat at constant pressure (J/kg.K).
ρ_l liquid density (Kg/m^3).
ρ_v vapor density (Kg/m^3).
P_{sat} saturation pressure (N/m^2).
P_a atmospheric pressure (N/m^2).
Pr Prandtle Number

where C_{sf}=0.0049 is the Rohsenow constant obtained from experimental data.**(Incropera et.al. (1990))**

The heat transfer of the falling liquid film is complex and depends on the magnitude of the heat flux applied at the evaporator. At a low evaporative heat flux a continuous liquid film is observed, a phenomena that is well described by Nusselt's condensation theory **(Incropera et.al. (1990))**. At a high evaporative heat flux, the film breaks down into droplets which start boiling and leads to a two phase fluid formed on the wall of the condenser. For the latter case, an empirical formulation for the heat transfer coefficient is:

$$h_f \frac{\left(\frac{\nu^2}{g}\right)^{\frac{1}{3}}}{k_l} = \left(\frac{4}{3}\right)^{\frac{1}{3}} Re_f^{\frac{-1}{3}} \quad (5)$$

$$Re_f = \frac{4 q_e x}{h_{fg} \mu} \quad (6)$$

$$x = L_p + \left(\frac{1}{2}\right) L_f \quad (7)$$

where
h_f film heat transfer coefficient ($W/m^2.K$).
x distance measured from the bottom of the thermosyphon (m).
L_p height of working fluid pool in the thermosyphon (m).
L_f distance from the top of the pool level to the top of the evaporator section (m).

IMPLEMENTED MODEL

The following assumptions are made:
1. The axial conduction along the length of the tube is negligible.
2. Constant heat flux is supplied to the evaporator.
3. Steady state operation with no heat losses.
4. The liquid pool level in the evaporator is assumed to be constant, implying that the rate of evaporation is equal to the rate of condensation.

The saturation pressure-temperature relationship used for both the liquid pool and the vapor just above the pool is expressed as:

$$p_v = 41.7548 - 0.281869 * T_{sat} + 0.00048 * T_{sat}^2 \quad (8)$$

Here T_{sat} is the saturated vapor temperature taken here from measurement adiabatic wall temperature.

The investigated variables are the heat flux and the vapor temperature inside the thermosyphon. Although the vapor is at its saturated pressure, the pressure varies along the height of the pool. The pressure at any point away from the bottom is given by:**(Shiraishi et. al. (1981))**

$$p(x) = p_v + \rho g (L_p - x) \quad (9)$$

Once pressure is known, the temperatures can be determined by the saturation temperature – pressure relation.

$$T_i(x) = \frac{1562}{(9.729 - \log(p(x)))}, \quad 0 \le x \le L_p \quad (10)$$

$$T_i(x) = \frac{1562}{(9.729 - \log(p_v))}, \quad L_p \le x \quad (11)$$

The heat flux at the condenser is calculated by:**(Siddharth 2011)**

$$q_c = q_e\left(\frac{L_e}{L_c}\right) \quad (12)$$

The heat transfer coefficients for different regions of the thermosyphon are calculated using equations (1), (3) and (4). The inner wall temperature $T_w(x)$ of the evaporator is calculated using the following relations:

$$T_w(x) = T_i(x) + \frac{q_e}{h_p}, \quad 0 \le x \le L_p \quad (13)$$

$$T_w(x) = T_i(x) + \frac{q_e}{h_f}, \quad L_p \le x \le L_e \quad (14)$$

at pool region, and liquid film region respectively.

At adiabatic region

$$T_w(x) = T_i(x), \quad L_e \le x \le L_e + L_a \quad (15)$$

while for condenser region

$$T_w(x) = T_i(x) - \frac{q_c}{h_c}, \quad L_e + L_a \le x \quad (16)$$

The outer wall temperatures are also calculated by:

At evaporator region

$$T_{woe}(x) = T_{wie}(x) + q_e A_{iwe}\frac{ln\left(\frac{d_o}{d_i}\right)}{2\pi k_w L_e} \quad (17)$$

At adiabatic region

$$T_{woa}(x) = T_{sat} \quad (18)$$

At condenser region

$$T_{woc}(x) = T_{wic}(x) - q_c A_{iwc}\frac{ln\left(\frac{d_o}{d_i}\right)}{2\pi k_w L_c} \quad (19)$$

where

T_{wie} inside wall temperature at evaporator (K).

T_{wic} inside wall temperature at condenser (K).

T_{sat} saturated vapor temperature (K).

T_i measured temperature at various locations (K).

Q_{in} input power (W).

Q_{out} output power (W).

k_w wall thermal conductivity of heat pipe (W/m.K).

A_{wie} evaporator inside surface area (m^2).

A_{wic} condenser inside surface area (m^2).

A_{woc} condenser outside surface area (m^2).

d_o outside diameter of heat pipe (m).

d_i inside diameter of heat pipe (m).

EXPERIMENTAL WORK

The test rig shown in Fig.(2) consists of a heater, a liquid reservoir for charging, a heat pipe, a cooling section, and also measuring instruments. The upper part of the heat pipe is equipped with a vacuum seal valve for connection to a mechanical vacuum pump and to the working fluid charging line. Simple blow-down by a vacuum pump with a rating of 10^{-2} Torr (1.333 pa) can easily remove the free gas from the heat pipe internal space. The vacuum pump was TINGWEI model TW-1A, supplied by Ting Wei Ji Dian, china. The removal of the adsorbed gas molecules is conducted through gradually heating heat pipe, while subjecting it to a vacuum at the same time. The maximum heating temperature should be above the maximum working wall temperature, which in this case was 375 K. This process is sometimes referred to as vacuum bake-out.

The details of heat pipe with fill tube, an electric heater for evaporator section, and a water jacket for condenser section are shown in Fig. (2).

The heat pipe consisted of a 1965 mm long copper tube having an inside diameter of 9.53 mm and outside diameter of 12.7 mm. The tube was sealed at one end and was provided with a vacuum valve at the other. The evaporator length 1.8m and adiabatic length of 0.6 m. The condenser section of the pipe consisted of a 0.145 m long (75 mm OD) concentric tube acting as cooling water jacket surrounding the pipe. An electrical resistance of a nominal power 1000 W, which was wrapped around the evaporator section, heated the evaporator section. To prevent the heat loss, the electric

elements were insulated by glass Wool having a thickness of 10 mm. Heat was removed from the condenser section by the water jacket as described.

The power supplied to the evaporator section was determined by monitoring the applied voltage and current using DT266C 3 1/2 DIGITAL CLAMP METER with voltage resolution is 0.1V, and its accuracy is ±0.8%. The current range was from 0.00 to 9.99 A with a resolution of 0.01 A, and accuracy of ±3.0%.

The volumetric flow rate through the condenser was measured by a rotameter of range (5 to 50 l/hr) model LZS-15 Wastewater (p.v.c flow meter), Yuyao Kingtai Instrument Co., Ltd. The Rotameter has an accuracy of 0.04 l/ hr. The rotameter was calibrated using a graduated container of 1 liter and a stop watch of 0.01 sec accuracy with flow rate range from 1- 50 l/ hr. In order to maximize the accuracy of the calibration process, it was repeated four times. The average error in flow rate measurement was estimated within ±1.5% at maximum flow rate of 10 l/ hr., while water inlet and outlet temperatures were measured using thermocouples type-k with an accuracy ±1 ^{o}C. The FC-72 was charged into the tube under 10^{-2} bar vacuum pressure. A variable voltage controlled the rate of heat transfer to the evaporator. Temperature distribution along the surface of the heat pipe was measured by thermocouples type-k within ± 0.5°C response. The thermocouples were mechanically attached to the surface of the pipe. The locations of the thermocouples are shown in table 1. The vapor temperature (Tv) was measured by thermocouple which attached to the surface of the adiabatic section. The upper surface of the thermocouple was fully insulated.

The rate of heat transfer to the evaporator section was calculated from the following relation:

$$Q_{in} = V.I \qquad (20)$$

The rate of heat removal from the condenser section was obtained from the following relation:

$$Q_{out} = \dot{m} C_p (T_o - T_i) \qquad (21)$$

The heat losses from evaporator and condenser sections were assumed to be negligible.

In order to find out the effects of input heat transfer rates and tilt angle on the thermal performance of the heat pipe, a series of tests were carried out for input heat transfer rate of (18, 28, 48, 63, 90W)

The effects of input heat transfer rate at various tilt angle (23, 45, 53, 74, 90^{o}) on the thermal performance of the heat pipe with constant filling ratio were investigated. Experiments were carried out with increasing input heat in the range of (18, 28, 48, 63, 90W) to the evaporator section. As a result, the average temperature of the surface of the evaporator section increased from 40 to 60^{o}C. Data were recorded until the system reached steady-state condition.

RESULTS AND DISCUSSION

Fig.(3) shows the wall temperature profile of the heat pipe at p=48 W, $\dot{m}$=0.0017 kg/s and θ= 90^{o}. The steady state is reached after (1500 s).

Figures (4) and (5) compares the axial wall temperature distribution along the heat pipe at various tilt angles with q=(18, and 90W) respectively,the results show that at low heat input, the wall temperature distribution shows a similar behavior for all tilt angles. At high heat input, a slight difference in the evaporator temperature was noticed. These results agree with those of **(Witwit (1998))**.

Figure (6) presents the variation of evaporator temperature with time for different tilt angles at low heat flux. It is obvious that the steady-state temperature is always higher at tilt angle of 90^{o} for which the steady-state evaporator temperature was about 38°C. For all given tilt angles considered, it is shown that the heat pipe at tilt angle of 53^{o} reached a steady-state evaporator temperature condition faster than other tilt angles. Higher temperature gradient was obtained at tilt angle 90^{o}.The same trend in evaporator temperature with

time at high heat flux is obtained as presented in Fig.(7). The steady-state temperature was 71°C at tilt angle of 53°. At tilt angle 45° the steady-state evaporator temperature is reached faster than other tilt angles. This indicates that drawing heat from the evaporator section is faster at tilt angle of 45°.

The variation of condenser temperature with time for heat pipe at low and high heat flux is presented in Figs. (8 and 9). The performance of a heat pipe would be better when the steady-state temperature of condenser is as close as possible to the steady-state evaporator temperature. The best performance is found when the heat pipe was positioned at an angle of 90°, by which its steady-state temperature reached a value of about 30 °C at low heat flux and 48°C at high heat flux. The heat pipe started with a low temperature gradient at low heat flux and high temperature gradient at high heat flux.

Fig.s (10 and 11) show the difference between evaporator and condenser temperatures with time. Lower temperature difference was obtained when heat pipe was at tilt angle of 23° and for low heat flux. At steady-state the temperature difference was about 8°C. Lower temperature difference was obtained when heat pipe was at tilt angle of 90° and high heat flux. At steady-state the temperature difference was about 18°C. This indicates that for the same amount of heat transfer rate, higher values of overall heat transfer coefficient can be obtained when tilt angle of heat pipe is 23° at low heat flux and 90° at high heat flux.

Fig. (12) illustrates the temperature distribution along the evaporator section above liquid pool surface (that is recorded by second, third and fourth thermocouples) is almost isothermal due to the existence of a continuous liquid film **(Semena et.al. 1978)** that covers the internal wall surface of the evaporator. During operation of the heat pipe, a liquid pool is present in the bottom of the evaporator zone and a thin liquid film flows down the remaining length of the heat pipe due to the effect of gravity. In the heat pipe, the heat transfer in the evaporator zone during steady –state operation of the heat pipe which is influenced by nucleate boiling and impulse convection, while the heat – transfer limit is caused by the onset of film boiling. As the heat input is increased, the heat pipe wall temperature rises too. The behavior in Figure is identical to the observations obtained by **(Andros 1980, EL-Genk et.al. 1999)**

At higher heat inputs, the temperature gradient at the evaporator-condenser interface becomes sharper and steeper. This represents the increased driving force between the evaporator and condenser sections as the evaporator temperature increases greatly relative to the condenser temperature. The temperature at the ends of the adiabatic section is affected by the evaporator and condenser temperatures, which proves that there is an axial heat transport through the wall in this section.

Comparison of Experimental Results With Empirical Correlations

Hong et.al. (2002) found out that nucleate boiling is the dominant mechanism in the evaporator, when the filling ratio is higher than 30%. Therefore, **(Shiraishi et. al. (1981))**and **(Rohsenow apude Noie (2003))** correlations based on nucleate boiling was chosen to compared with experimental data. Rohsenow correlation is adopted in this study since the comparison performed between the experimental results and the Shiraishi and Rohsenow correlations shows that the latter give nearest results as shown in Fig.(13) especially at low input heat flux.

From the measured data on wall temperature distribution, vapor temperature and value of thermal load, the heat transfer coefficient in the evaporator can be evaluated using the following equation:

$$h_{exp} = \frac{Q_{in}}{\pi d_o L_e (\bar{T}_e - T_v)} \quad (22)$$

where

$$\bar{T}_e = \frac{T_1 + T_2 + T_3 + T_4}{4} \quad (23)$$

Validation of Model

Shiraishi's model for heat pipe wall temperature and working fluid temperature was implemented and validated with experimental data. A vapor temperature of the working fluid was used as the same temperature of adiabatic wall from experimental measurements. Figure (14) shows the temperatures for a filling ratio = 0.7 ,input heat flux 1253 W/m^2,tilt angle=90^o and mass flow rate=0.0017 Kg/s. The temperature of the working fluid inside the heat pipe is equal to the saturation temperature 62 ^{o}C in both the adiabatic section. Therefore the saturation pressure inside adiabatic and the condenser section can be calculated from equation(8), pressure of working fluid increases with the depth, which in turn leads to a higher temperature down the length of the evaporator; this is shown clearly by the linearly increasing temperature from height 1300 mm to 0mm (bottom of the evaporator). It can be seen from the figure that the model agrees well with the experiments.

Figure (15) shows the temperatures for a filling ratio = 0.7, heat flux 250 W/m^2,tilt angle=90^o and mass flow rate=0.0017 Kg/s .The model wall temperature are much closed with model fluid temperature because the amount of heat flux were applied along the length of the evaporator are very small. It can be seen from the figure that the model not agrees well with the experiments in this range.

CONCLUSIONS

The effects of input heat flux on the heat transfer characteristics of a vertical closed two-phase heat pipe under normal operating conditions was investigated for a range of input heat flux 250W/m^2<q<1253W/m^2 and various tilt angle. The following conclusions have been extracted:

1. The temperature distribution along the evaporator wall in the evaporator section was almost isothermal. The measured temperature along the condenser showed lower values. This drop of temperature is expected because of the internal resistances due to boiling and condensation.
2. The simulation results show the necessity of an experimental study in order to generate trustworthy correlations for both evaporator and condenser regions of heat pipe since the previous published correlations show great divergence with correlations obtained by Nusselt.
3. The heat transfer coefficient of the evaporator showed a trend that increased with the increase of the power.

REFERENCES

Andros F.E.; Heat transfer characteristics of the two-phase closed thermosyphon (wickless heat pipe) including direct flow observation; Ph.D. Dissertation, Arizona State University,1980.

Azada E., Mohammadieha F., Moztarzadeh F. ;Thermal performance of heat pipeheat recovery system; Journal of Heat Recovery Systems;1985; V. 5 (6): pp. 561-570.

Basran T., Kücüka S.; Flow through a rectangular thermosyphon at specified wall temperatures; International Communications in Heat and Mass Transfer; 2003;V. 30 (7) :pp. 1027–1039.

El-Genk M.S., Saber H.H.; Determination of operation envelopes for closed two-phase thermosyphons; Int. J. Heat Mass Transfer; 1999;V.42(5):pp.889–903.

Faghri A.; Heat pipe science and technology; First edition; Taylor & Francis, ISBN 978-1560323839, New York USA; 1995.

Fu H.D., Pei G., Ji J., Long H., Zhang T., Chow T.T.; Experimental study of a

photovoltaic solar-assisted heat-pump/heat-pipe system; Applied Thermal Engineering 40 (2012) 343-350.

Gershuni A., Nishchik A., Pysmennyy Y., Polupan G., Sanchez-Silva F., Carvajal-Mariscal I; Heat exchangers of the gas-gas type based on finned heat pipes; International Journal of Heat Exchangers; 2004;V.5 (2): pp. 347-358.

Hong S.H., Kim C.J., Park Y.J., Kang H.K.; An experimental study on the heat transfer characteristics of a FC-72 thermosyphon; 12th International Heat Pipe Conference, Moscow; 2002: pp. 308–314.

Incropera F., DeWitt D.; Fundamentals of heat and mass transfer; 3rd Edition, John Wiley and Sons, Inc., 1990.

Jialun H., Tongze M., Zhengfang Z.; Investigation of boiling liquid pool height of a two-phase closed thermosyphon; Proceeding ofthe Eighth International Heat Pipe Conference; Beijing China 1992: pp. 154–159.

Jiao B., Qiu L.M., Zhang X.B., Zhang Z.; Investigation on the effect of filling ratio on the steady-state heat transfer performance of a vertical two-phase closed thermosyphon; Applied Thermal Engineering ; 2008; V.28 (11):pp.1417–1426.

Nemec P., Čaja A., Malcho M.; Mathematical model for heat transfer limitations of heat pipe; Mathematical and Computer Modelling 57 (2013) 126–136.

Nkwetta D.N., Smyth M., Zacharopoulos A., Hyde T.; In-door experimental analysis of concentrated and non-concentrated evacuated tube heat pipe collectors for medium temperature applications; Energy and Buildings 47 (2012) 674–681.

Noie S.H; Heat transfer characteristics of a two-phase closed thermosyphons ; Applied Thermal Engineering; 2005; V.25(4): pp. 495-506.

Noie S.H., Kalaei M.H. , Khoshnoodi M; Experimental investigation of a two phase closed thermosyphon; The 7th International Heat Pipe Symposium; 2003, October 12-16, Jeju, Korea.

Park J., Kang K., Kim J. ;Heat transfer characteristics of a two-phase closed thermosyphon to the fill charge ratio; International Journal of Heat and Mass Transfer;2002; V.45,(23): pp. 4655-4661.

Peterson G.P; An introduction to heat pipe modeling, testing, and applications; John Wiley& Sons, Inc., ISBN 978-0471305125, New York USA; 1994.

Pioro I.L.; Experimental evaluation of constants for the Rohsenow pool boiling correlation; International Journal of Heat and Mass Transfer;1998; V. 42(11): pp. 2003-2013.

Reay D.A; A review of gas-gas heat recovery systems; Journal of Heat Recovery Systems; 1981; V.1 (1): pp. 3-41.

Semena M.G. and Gerahmi A.N.; Investigation of the maximum heat transport capacity of heat pipe with matel fiber wicks; Teplofiz. vys. temp. 1978,16(5):pp.1060-1068.

Shiraishi M., Kikuchi K., Yamarcishi T.; Investigation of heat transfer characteristics of a two phase closed thermosyphon; Heat Recovery Systems;1981; V.1: pp. 287 – 297.

Streltsov A.I.; Theoretical and experimental investigation of optimum filling for heat pipe; Heat Transfer Soviet Res; 1975; 7 (1):pp.23–27.

Witwit A.M.; A study of the gravity assisted and variable conductance heat pipes with an internal wall separating liquid and

vapor phases; Ph. D. Thesis, Mech. Eng. Dept., College of Engineering, University of Baghdad, 1998.

Zuo Z.J., Faghri A. ;A network thermodynamic analysis of the heat pipe; International Journal of Heat and Mass Transfer;1998; V.41(11): pp. 1473-1484.

Table (1): Thermocouple Locations Along Heat pipe

Thermocouple No.	1	2	3	4	5	6	7	8	9	10	11
Location (mm)	200	700	1200	1700	1810	1830	1860	1890	1020	Water inlet	Water outlet

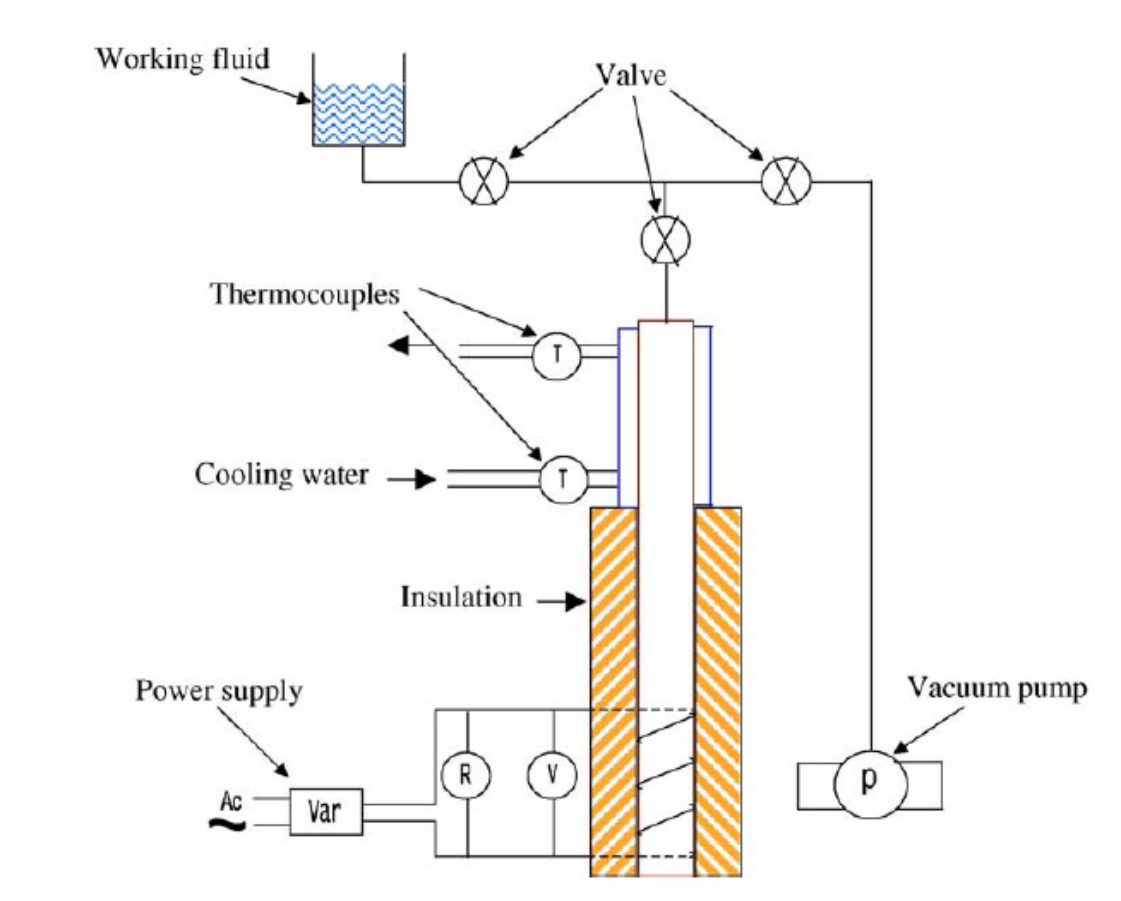

Fig.(1): Schematic of The Test Rig.

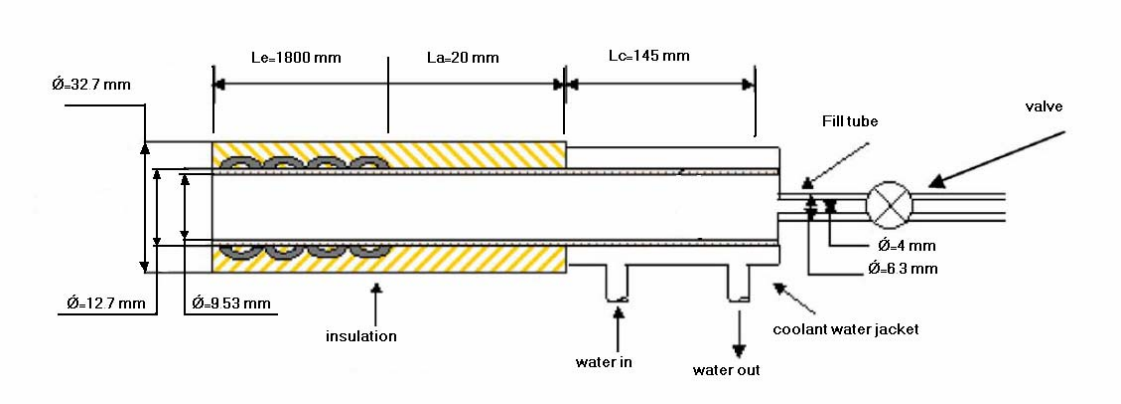

Fig.(2): Details of Heat pipe.

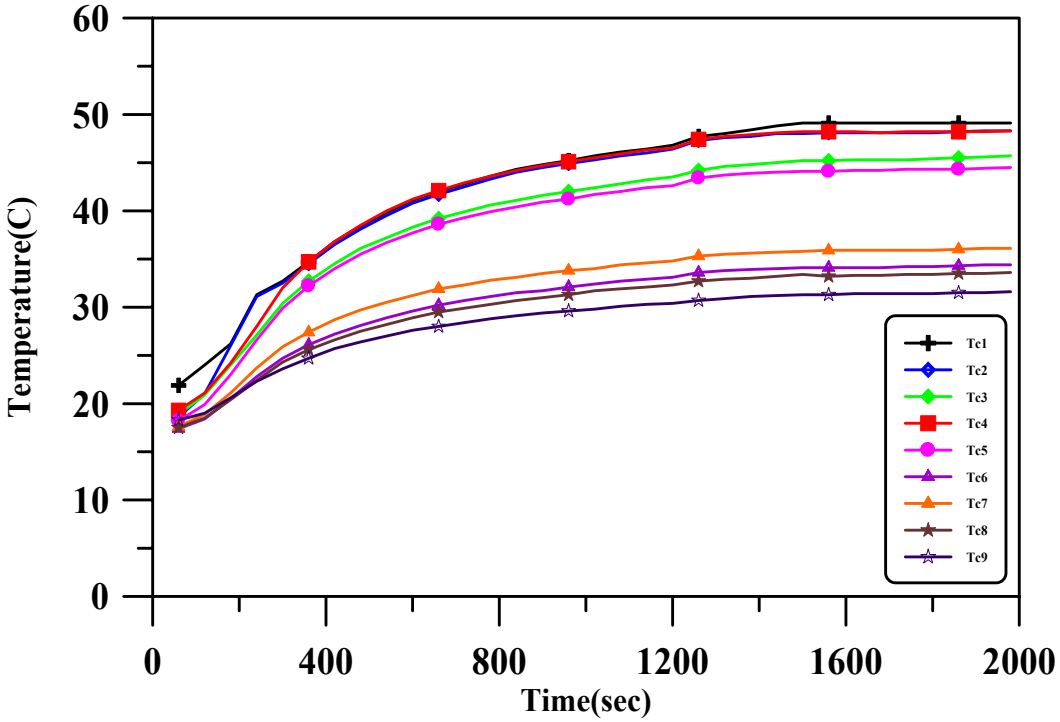

Fig. (3): Time Response of Thermocouples With P=48 W, $\dot{m}$=0.0017 Kg/s, θ= 90°

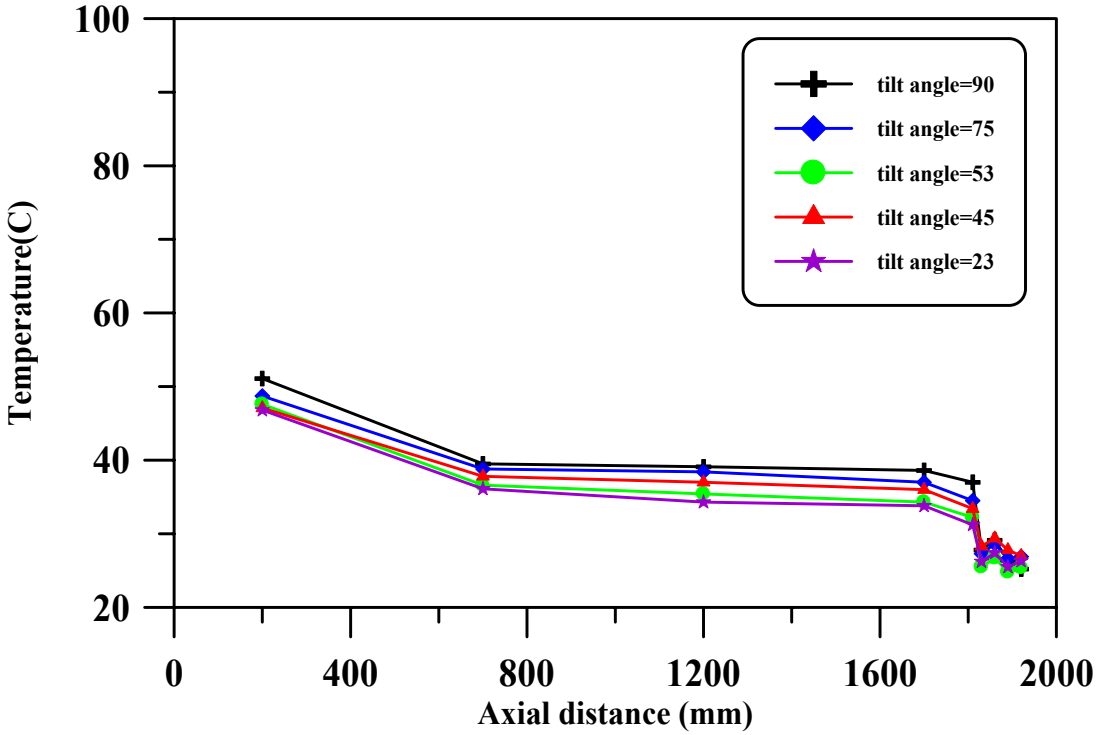

Fig.(4) Axial Wall Temperature Distribution Along Heat Pipe at Various Tilt Angle with P=250 W/m^2, m$^{\bullet}$=0.0017Kg/s.

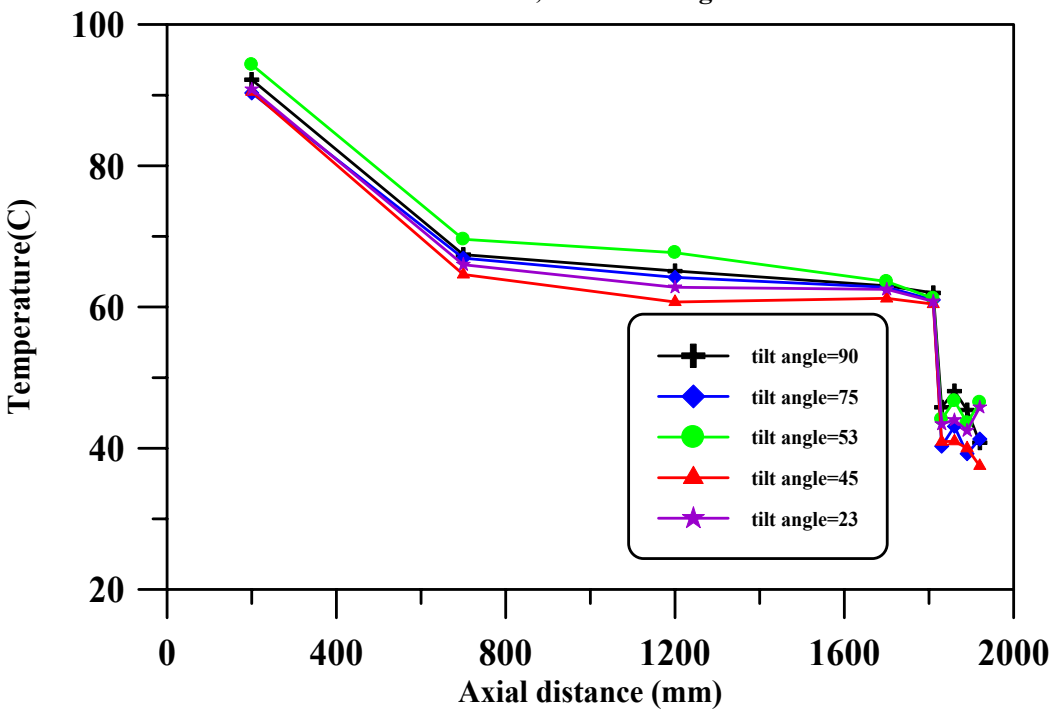

Fig.(5) Axial Wall Temperature Distribution Along the Heat Pipe at Various Tilt Angle with P=1253 W/m^2, m$^{\bullet}$=0.0017 Kg/s.

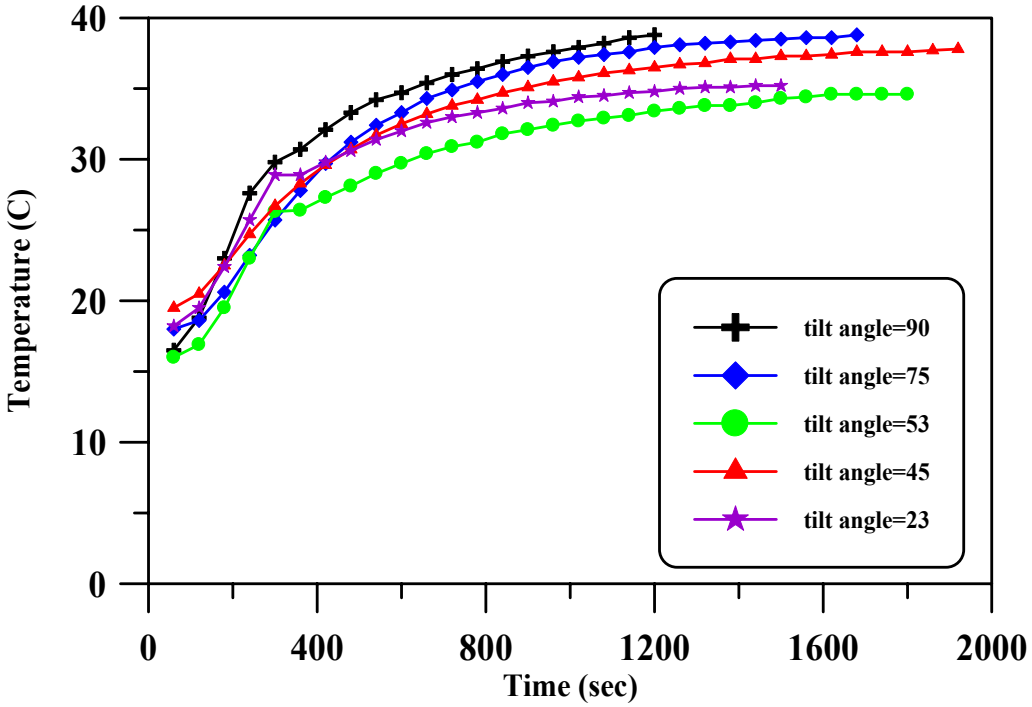

Fig. (6): Variation of Evaporator's Temperature With Time for Different Tilt Angles at Low Heat Flux.

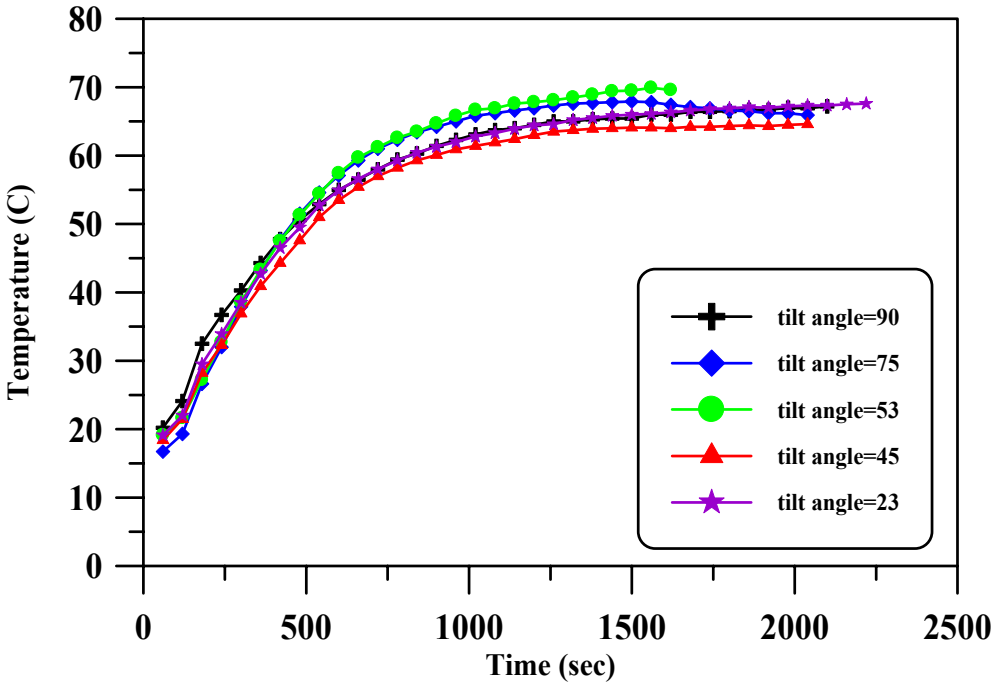

Fig.(7): Variation of Evaporator's Temperature With Time for Different Tilt Angles at High Heat Flux.

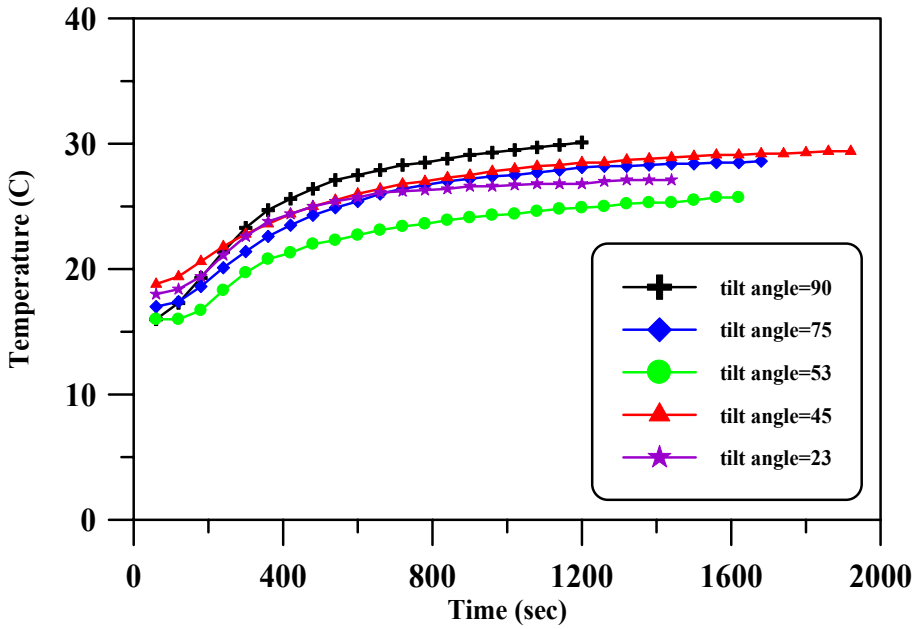

Fig.(8)Variation of Condenser's Temperature With Time for Different Tilt Angles at Low Heat Flux.

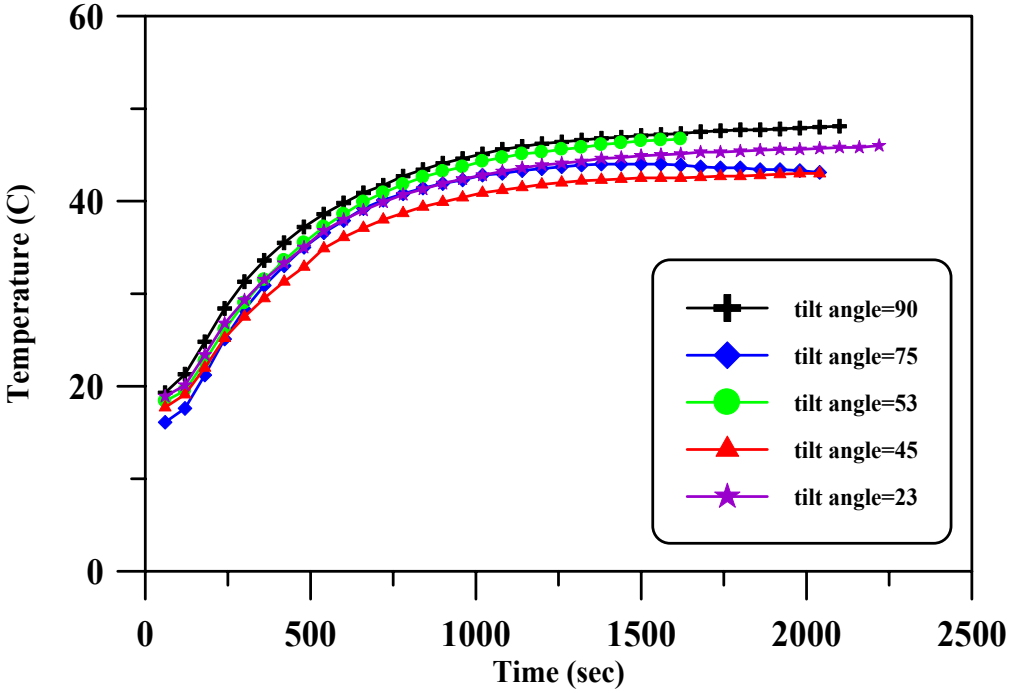

Fig.(9)Variation of Condenser's Temperature With Time for Different Tilt Angles at High Heat Flux.

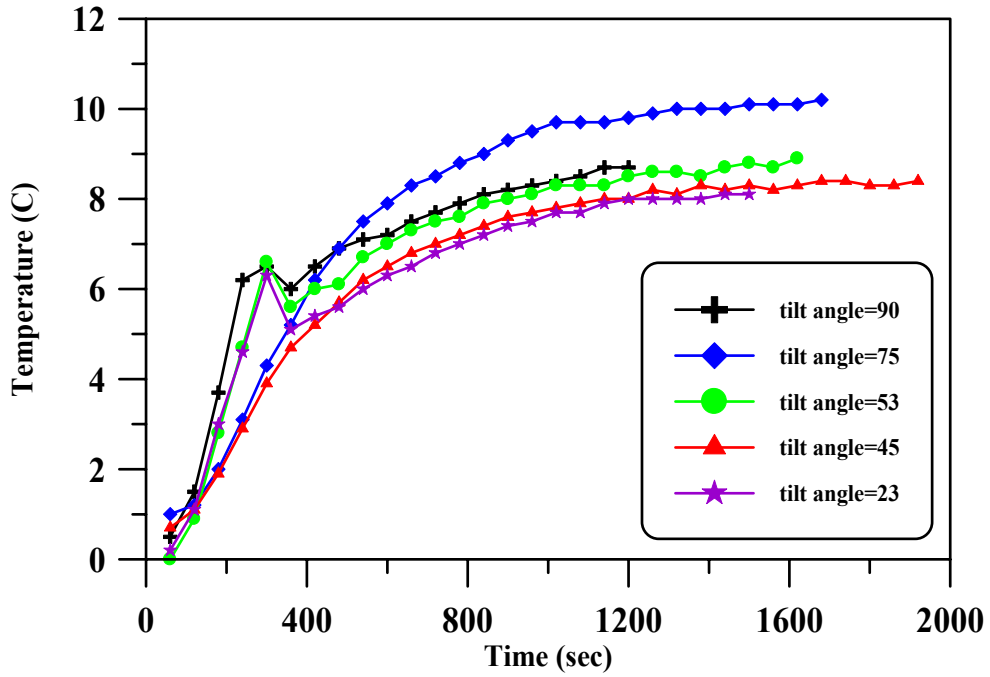

Fig.(10) Variation of the Difference Between Evaporator and Condenser Temperatures With Time for Different Tilt Angles at Low Heat Flux.

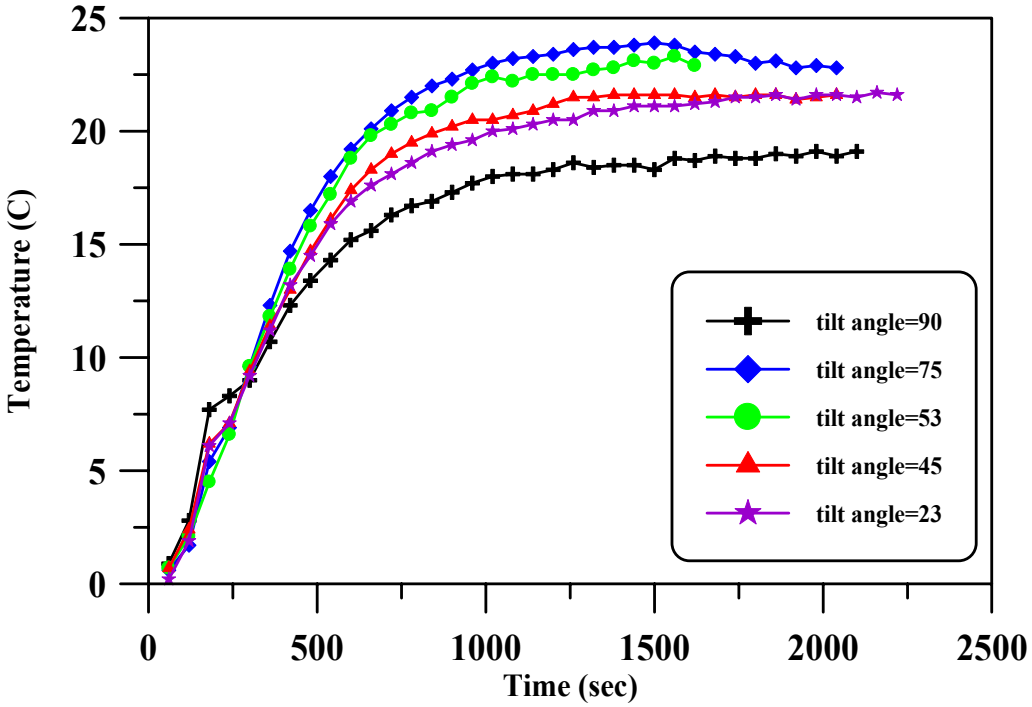

Fig.(11) Variation of the Difference Between Evaporator and Condenser Temperatures With Time for Different Tilt Angles at High Heat Flux.

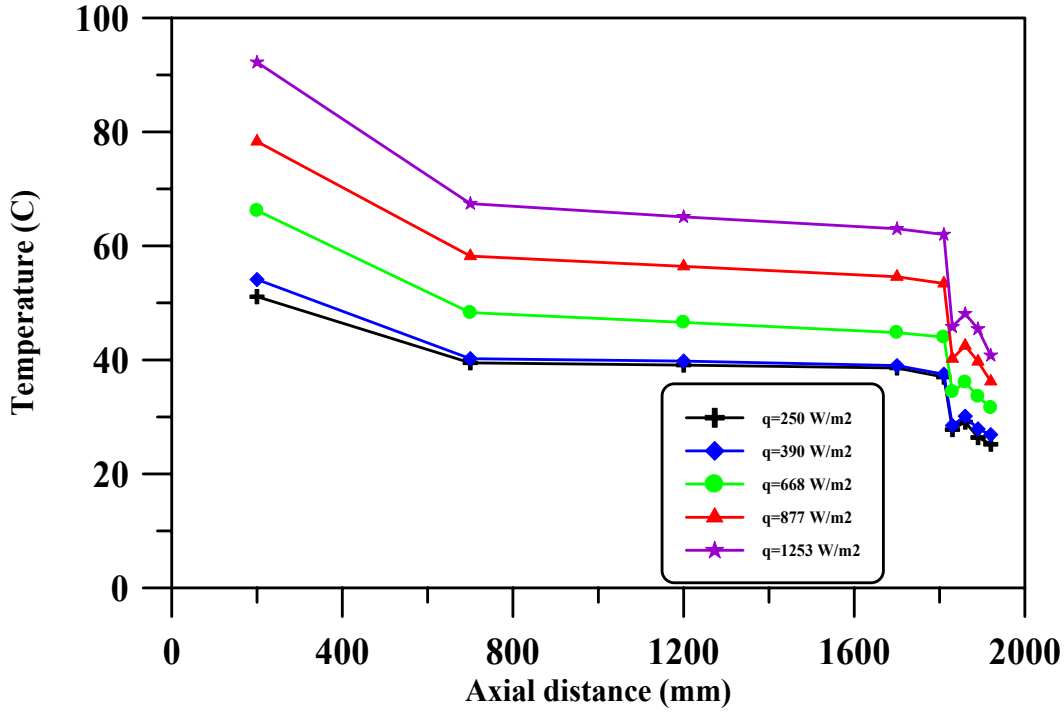

Fig.(12): Temperature Variations Along the Heat Pipe at Different Inlet Heat Flow Rates at (θ=90^o and FR=0.7).

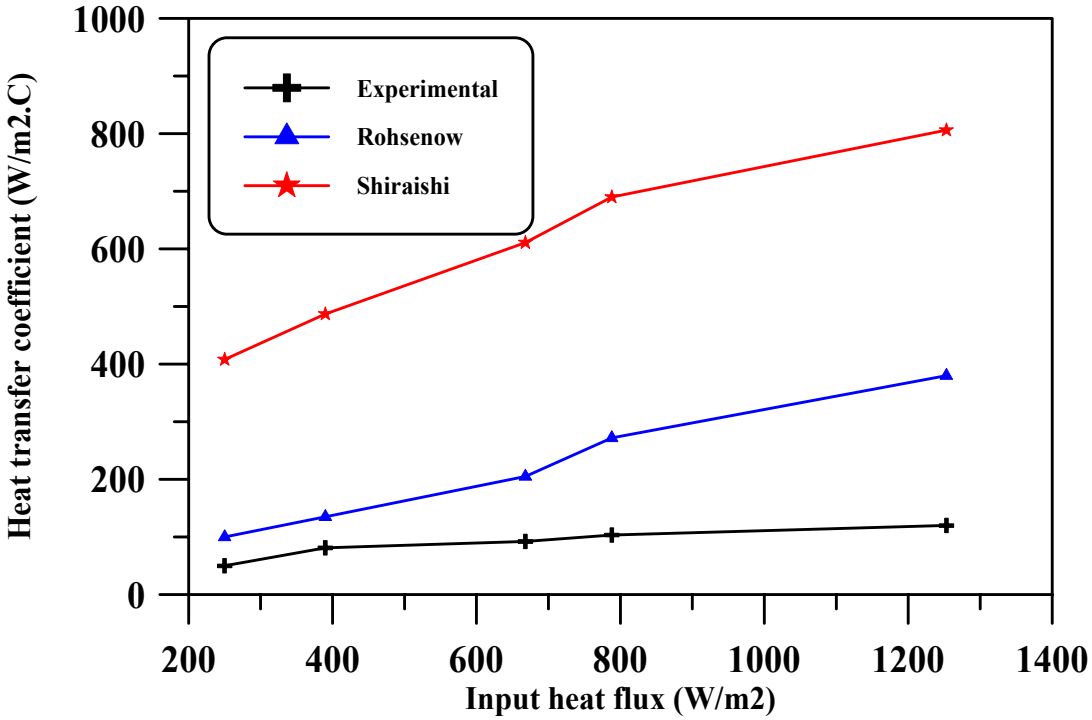

Fig(13) Heat Transfer Coefficient vs. Heat Flux Input for FR=70%

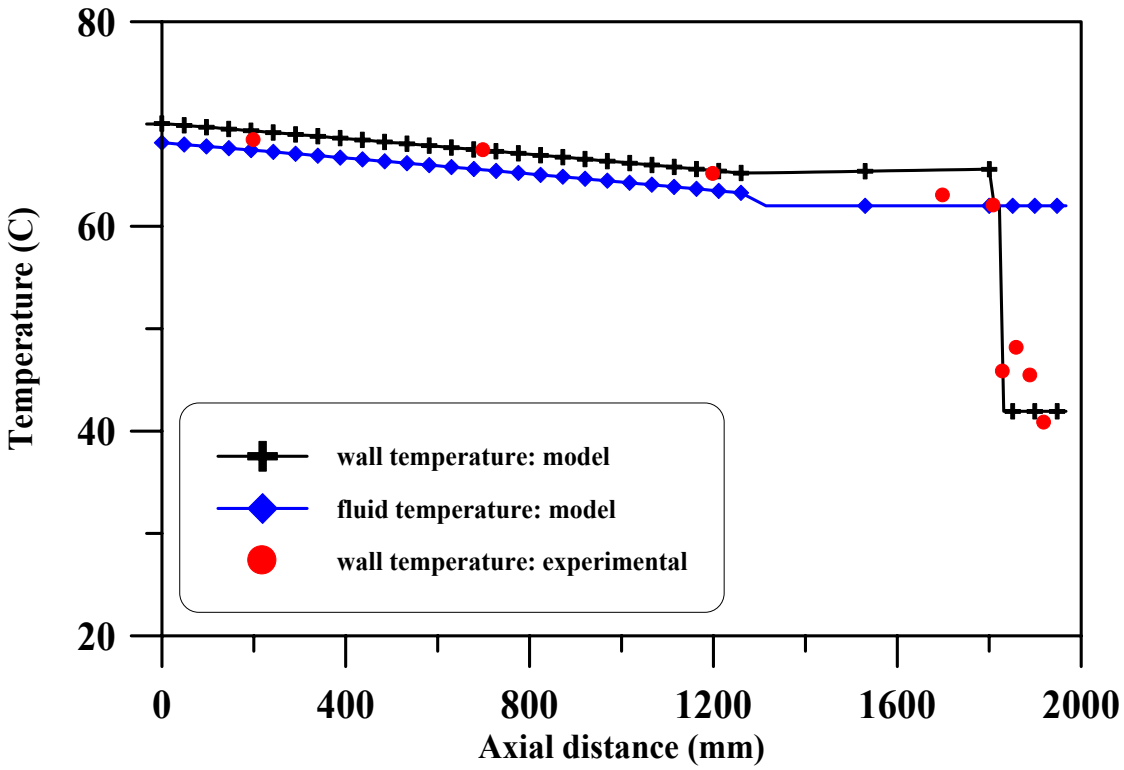

Fig (14) Temperature Profile of Working Fluid and Wall for FR=0.7 and Input Heat Flux=1574 W/m^2.

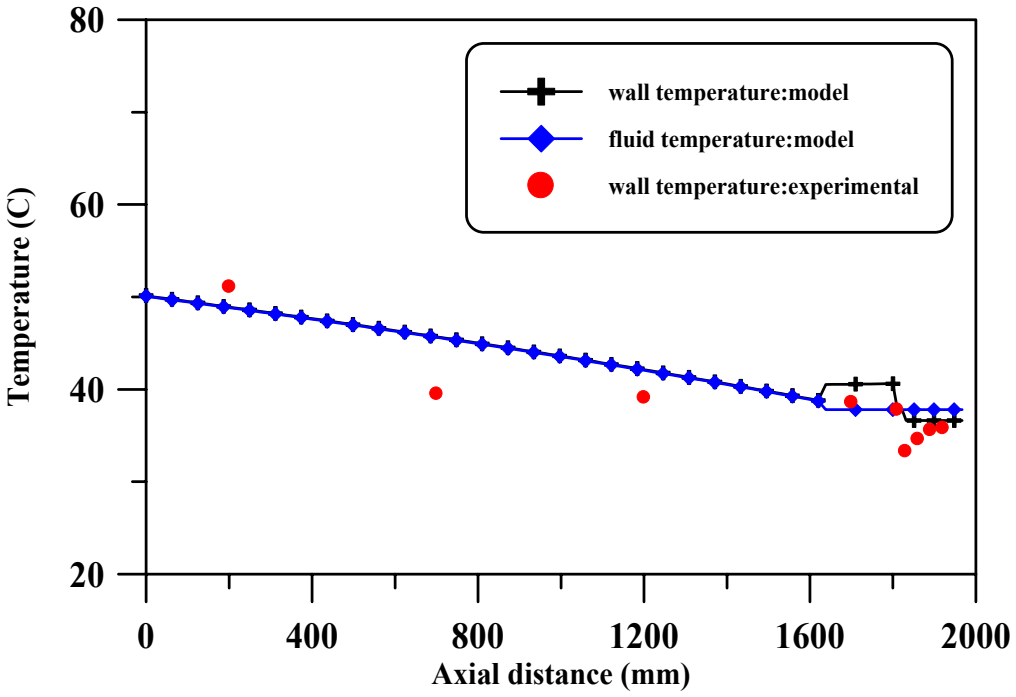

Fig. (15): Wall and Working Fluid Temperature Profile at Input Heat Flux=250 W/m^2.

NOMENCLATURE

Symbols			
A	surface area (m^2).	k	thermal conductivity (W/m.K).
C_p	specific heat at constant pressure (J/kg.K).	L	length (m).
C_{sf}	constant that depended upon the nature of the surface–fluid combination.	P	pressure (N/m^2).
		Q	power (W).
d	diameter (m).	q	heat flux (W/m^2).
g	gravitational acceleration (m/s^2).	Re_c	film Reynolds number (Kg/N).
h	heat transfer coefficient ($W/m^2.K$).	T	temperature (K).
h_{fg}	latent heat of vaporization (J/kg).	x	distance measured from the bottom of the thermosyphon (m).
Greek symbols			
ν	kinematic viscosity $=\mu/\rho$ (m^2/s).	ρ	density (Kg/m^3).
μ	dynamic viscosity ($N.s/m^2$).	θ	tilt angle (o).
Subscripts			
a	atmospheric	l	liquid
c	condenser	o	outside
e	evaporator	out	Output
f	film	p	pool
i	inside	sat	saturation
in	input	v	vapor
		w	Wall